ELF/VLF recordings during the 11 March 2011 Japanese Tohoku earthquake

M. B. Cohen[1] and R. A. Marshall[1]

Received 22 April 2012; revised 15 May 2012; accepted 16 May 2012; published 9 June 2012.

[1] Broadband ELF/VLF radio recordings (0.2–40 kHz) were made at a site in Onagawa, Japan located ∼102 km from the epicenter of the M9.0 11 March 2011 earthquake, the fifth most powerful earthquake in recorded history. The receiver operated for about two minutes after the start of the earthquake, after which the receiver lost power. Examination of the VLF data shows no radio emissions preceding or coincident with the onset of the earthquake. However, once the secondary seismic waves reached the receiver, a number of impulses and diffuse noise bands arose which may result from the entire power grid shaking or from radio emissions from compressing rocks. Examination of the ELF data (0.2–1 kHz) show no precursor effect in the hours preceding the earthquake. Examination of VLF data from narrowband transmitters shows no anomalous activity in the days or weeks preceding the earthquake. Our instrument low-frequency cut-off is ∼200 Hz, and thus we cannot comment on emissions in the ULF range (<10 Hz). **Citation:** Cohen, M. B., and R. A. Marshall (2012), ELF/VLF recordings during the 11 March 2011 Japanese Tohoku earthquake, *Geophys. Res. Lett.*, *39*, L11804, doi:10.1029/2012GL052123.

1. Introduction

[2] Beginning in the 1980s, there have been reports of electromagnetic emissions and anomalies as precursors to earthquakes, either in the Ultra Low Frequency range (<10 Hz) or in the Extremely Low Frequency and Very Low Frequency range (ELF/VLF, 0.3–30 kHz). *Fraser-Smith et al.* [1990] detected a large increase in ULF radio noise (most pronounced at 0.1 Hz) in the days and hours before the M8.9 Loma Prieta earthquake outside San Francisco, but did not detect a precursor signal in the ELF/VLF data, despite having a receiver only 50 km from the epicenter. The receiver lost power at the onset of the earthquake, so data during the earthquake itself were not available. *Goghberg et al.* [1982] detected a number of ELF, VLF and LF emissions prior to earthquakes between M5 and M7 in the USSR.

[3] There have also been some efforts to detect ELF/VLF waves emitted prior to earthquakes, aboard orbiting satellites. *Parrot and Mogilevskii* [1989] detected ELF/VLF signals and intensity increases in the sporadic-E layer, using measurements from the GEOS-2 and AUREOL-3 satellites. However, other investigations have found no connection between earthquakes and ELF/VLF emissions [*Rodger et al.*, 1996], or found a weak decrease in ELF/VLF signal amplitudes detectable only through statistical averaging [*Němec et al.*, 2009].

[4] Yet another proposed method for earthquake prediction is from subionospheric propagation of VLF transmitters [*Gokhberg et al.*, 1989], which act as probe waves for the lower ionosphere. Using the signature of a VLF transmitter at the day/night transition, a series of studies [*Hayakawa et al.*, 1997; *Molchanov and Hayakawa*, 1999] have stated that the apparent minimum group delay or amplitude point during the sunrise terminator shifts in the days before an earthquake, due to a VLF ionospheric reflection height change of 1.5 km. However, subsequent analysis have not been able to demonstrate that these terminator shift can be linked to earthquakes with statistical significance [*Clilverd et al.*, 1999].

[5] Most of the aforementioned efforts are hampered by the rarity of earthquakes (particularly those with high magnitude), and by the fact that other natural drivers of ULF/ELF/VLF signals can also be imposed onto the data (particularly from lightning and geomagnetic activity), which have similar geomagnetic effects (ULF/ELF emissions, and ionospheric disturbances detectable in VLF narrowband transmitter data). To date, earthquakes cannot be reliably forecast, including via seismology, and the goal of earthquake forecast remains an elusive one.

[6] We present here the first record of broadband ELF/VLF radio emissions made during an exceptionally strong earthquake close to the epicenter (∼100 km). Given the rarity of such powerful earthquakes, the uncertain locations where the epicenters will lie, plus the surprising fact that the receiver continued to operate through the initial stages of the earthquake, the measurements presented here are a unique and highly fortuitous window into the ELF/VLF environment before and during the most serious and damaging earthquakes.

2. Data

[7] On 11 March 2011, at 05:46:24 UT, an earthquake with magnitude 9.0 occurred off the coast of Japan, at a depth of 30 km, with its epicenter at 38.297°N, 142.372°E, and lasting six minutes. It is the fifth most powerful earthquake since 1900, when earthquake monitoring became more prevalent and sophisticated. The earthquake, hereafter referred to as the "Tohoku earthquake" caused extensive damage across Japan, both from the earthquake and from a subsequent tsunami.

[8] In the months leading up to the Tohoku earthquake, an ELF/VLF radio receiver was operating near Onagawa, Japan (38.44°N, 141.22°NE), ∼102 km from the epicenter. Figure 1

[1]Department of Electrical Engineering, Stanford University, Stanford, California, USA.

Corresponding author: M. B. Cohen, Department of Electrical Engineering, Stanford University, 350 Serra Mall, Room 356, Stanford, CA 94305, USA. (mcohen@stanford.edu)

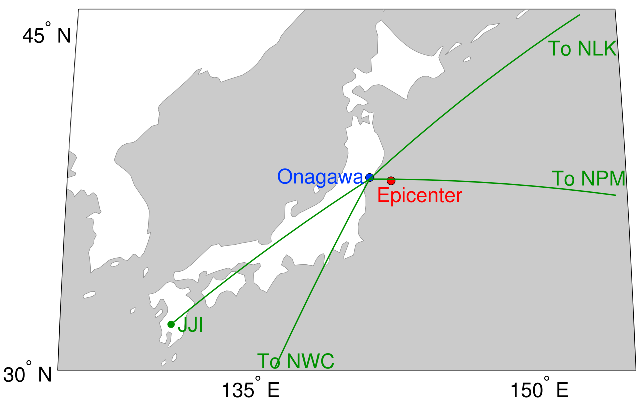

Figure 1. Map of the earthquake epicenter and receiver location, as well as the paths to four VLF transmitters.

shows the location of the receiver as well as the epicenter of the Tohoku earthquake.

[9] The receiver consisted of two orthogonal air-core loop antennas, sampling the two horizontal components of the magnetic field, at 100 kHz, with 16 bit sampling. The sensitivity of the receiver allows detection of signals down to the few fT/Hz$^{\frac{1}{2}}$ range. The receiver was GPS-synchronized to provide 100 ns timing accuracy. Details of the receiver design are described by *Cohen et al.* [2010a]. The receiver has a strict lower frequency cutoff of ~200 Hz, and an upper cutoff of ~47 kHz.

[10] Although Japan is a well-known seismically active region, the receiver was not set up for the purposes of studying earthquakes, but it was serendipitously operating before and during the Tohoku earthquake. As described by *Cohen et al.* [2010a], the receiver records two types of data: (1) broadband data, which cover the full spectrum between 200 Hz and 50 kHz, are preserved only for a buffer period extending a few days prior at any given time, due to the large storage requirement (1.5 GB/hour), and (2) narrowband data, which are the amplitudes and phases of VLF transmitter signals, which can be used as a remote sensing tool for the lower ionosphere, and are usually saved continuously.

[11] The Tohoku earthquake initiated at 05:46:24.12 UT, at a depth of 30 km, and lasting about six minutes. The depth of the ocean at the epicenter is ~990 m. The first seismic p-waves reached the location of the receiver at about 05:46:45 UT and the more destructive seismic s-waves reaching the location of the receiver at about 05:46:58 UT, based on approximate propagation velocities of 5.5 km/sec and 3.3 km/sec, respectively [*Kennett and Engdahl*, 1991]. Remarkably, the ELF/VLF receiver continued to record until 05:48:19, at which point the power to the computer was lost. The recordings thus ran until 115 seconds after the earthquake began, or 87 seconds after the s-waves reached the receiver. The powerful tsunami that followed the Tohoku earthquake took a minimum of 10 minutes to reach the coastline, well after our data recordings ended.

3. Observations

3.1. Broadband VLF

[12] Figure 2 shows one second of VLF data during the onset of the Tohoku earthquake, with the vertical dashed line indicating the start time. The units in the colorscale are logarithmic, with respect to an arbitrary magnetic field amplitude. The horizontal lines in the spectrogram are VLF transmitters, to be discussed later. The spectrogram also contains a large number of impulsive (~1 ms) radio atmospherics, or sferics, which originate from lightning events at long distances, and appear as thin vertical lines. Sferics are consistently present in ELF/VLF recording, typically with rates of dozens per second, originating from anywhere on Earth. The frequency content of a sferic evolves with distance due to propagation in the Earth-ionosphere waveguide. Had there been VLF emissions from the earthquake that escaped the seawater, they would have propagated to the VLF receiver very rapidly (on a time scale of ms). Although the evidence for >200 Hz emissions prior to or in association with earthquakes is weak in general, this premise for this particular case is made even more unlikely by the fact that the epicenter was deep underneath conducting seawater, which attenuate radio waves with exponential decay at the skin depth ($\delta \sim 17.8$ m for $\sigma = 4$ S/m and $f = 200$ Hz).

[13] There is a cluster of sferics that occurs between 300–450 ms after the start of earthquake, but the frequency content and spacing of those sferics are consistent with multiple return strokes from a single distant lightning flash. The frequency content is not consistent with a nearby (102 km) impulsive source. As such, we conclude that there is no anomalous impulsive emission associated with this earthquake in VLF data that can be detected at a range of 100 km. In this spectrogram, we have removed interference from 50 Hz power lines using the tracking filter technique described by *Cohen et al.* [2010b]. The weak remaining residual energy between 1 and 2 kHz is from local noise sources, and is not associated with anything seismic.

[14] Figure 3 shows the lower 10 kHz of data for the last 139 seconds of recordings (beginning at 05:46 UT), including the beginning of the Tohoku earthquake. The horizontal lines are interference from power lines, at 50 Hz and its harmonics, which have not been removed in this record. The time of the earthquake was 05:46:24.12 UT, or ~24 seconds into the plot, and is indicated with a vertical white dashed line. The gray and black lines show the estimated arrival times of the p-wave and s-wave, assuming

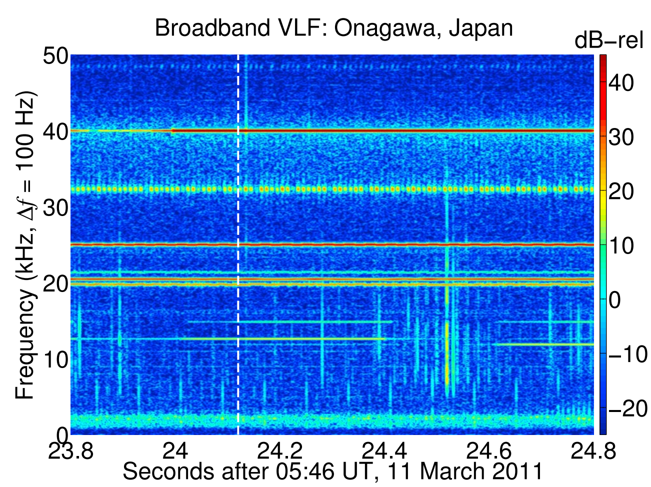

Figure 2. One second of VLF data during the onset of the earthquake. The vertical dashed white line indicates the start time of the earthquake, or 05:46:24.12.

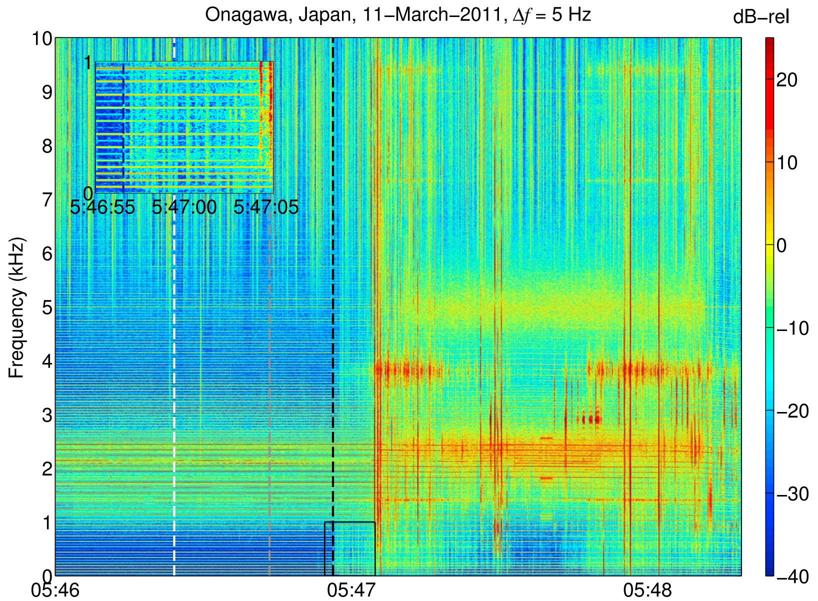

Figure 3. VLF Data during the last 199 seconds of operation. The vertical line indicate the start of the Tohoku earthquake (white) and the estimated arrival times of the p-wave (gray) and s-wave (black) at the receiver. The thumbnail in the top left is a zoom-in of the lower 1 kHz around the arrival of the s-wave, indicated with a black box in the main spectrogram.

propagation speeds of 5.5 km/sec and 3.3 km/sec, respectively, and propagating along a straight line path from a depth of 30 km.

[15] The arrival of the p-wave does not seem to be associated with any anomalous activity, although there may be a few impulses arriving in the few seconds before the s-waves arrive, between 100–1000 Hz. The arrival of the s-waves brings several clear features to the recordings. First, a series of weak impulses begin at 05:46:56 UT, lasting approximately ten seconds, with the bulk of their energy <2 kHz. The impulses are frequent enough to make the appearance in the spectrogram of the entire background noise level rising. The thumbnail in the top left corner of Figure 3 shows the lower 1 kHz of the spectrogram, during the time when the s-wave arrives, as marked by the black box in the main spectrogram. In this zoom-in, the impulses in the data can be clearly seen, along with a modest rise in the overall background noise level.

[16] About 8 seconds after the arrival of the s-wave, a few very intense impulses are observed and are accompanied with a significantly strengthened band of noise between 3.5 and 4.0 kHz, another between 4.5 and 5.5 kHz, and a third near 9.5 kHz. The weaker noiseband between 4.5 and 5.5 kHz lingers consistently for roughly a minute, whereas the other two noisebands weaken and then re-intensify. None of the aforementioned impulses or noisebands appear to be present in the hours prior to the earthquake. There is additional bizarre activity than we cannot really describe concisely, so we instead refer to the figure which largely speaks for itself.

[17] It should be emphasized that we have no way of knowing empirically whether any of these anomalies were a result of rock stresses as the seismic waves passed generating waves via the piezoelectric effect, or whether they resulted from the shaking of nearby buildings and power lines, although the receiver was not in a densely populated area. Resolution of this may be left to future workers, although we lean here towards the explanation that the anomalous emissions (both impulsive and diffuse) somehow resulted from physical shaking and vibrations of buildings and power lines (as well as the VLF antenna). However, the seismoelectric effect has been observed to emit diffuse noise bands at these frequencies, for instance from sand [*Bordes et al.*, 2006], and thus we cannot rule out a source at or just below the surface. We do note one piece of evidence supporting the possibility of a piezoelectric source. The aforementioned broadband impulses below 2 kHz appears to have been timed with the arrival of the s-waves, rather than with the most significant stressing of the power grid as reflected in the power line frequency, which we now discuss.

[18] Figure 4 shows a zoomed-in spectrogram of the last 120 seconds before the receiver lost power. The horizontal striations are harmonics of 50 Hz (the power grid

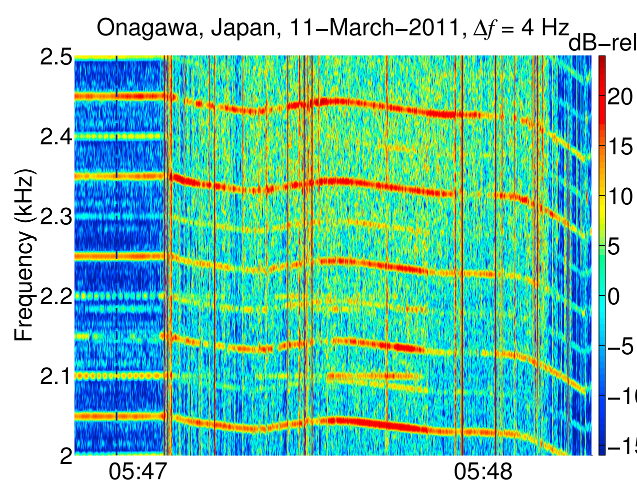

Figure 4. Power line interference during the last 120 seconds of operation. The vertical black line indicates the estimated arrival time of the s-wave at the receiver.

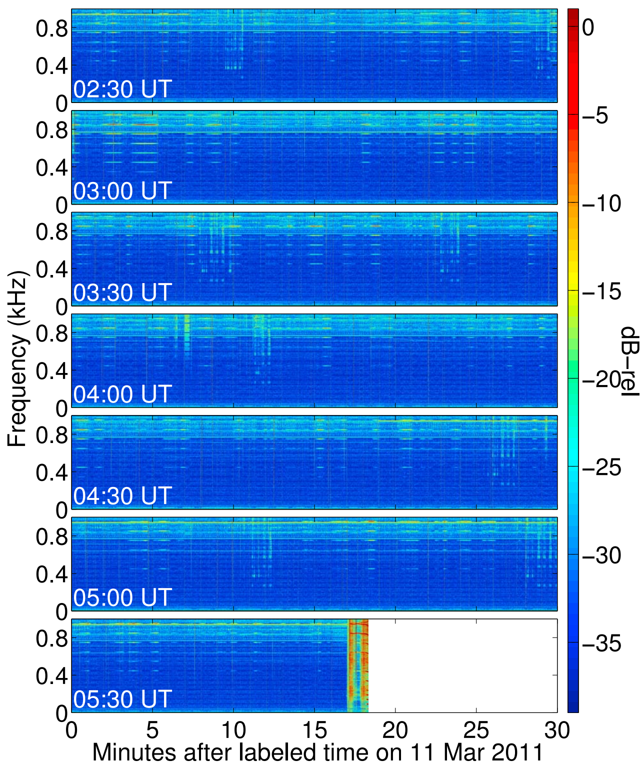

Figure 5. Lower 1 kHz of spectrograms for last 3+ hours before earthquake.

frequency), which are regular features of ELF/VLF data if they are taken anywhere near power lines. Typically, the odd numbered harmonics are stronger than the even numbered harmonics, and the fundamental frequency stays close to 50 Hz, oscillating only slightly (<0.1 Hz) in response to changing loads on the power grid. In this case, the fundamental power line frequency drops and then undulates during the 87 seconds after the s-wave reached the receiver. The fundamental 50 Hz frequency dropped by as much as ~0.7 Hz during this time. Furthermore, the power line harmonics appear to divide and undulate in intensity. These characteristics appear to be a result of the electrical stressing and eventual failure of the power grid, leading to a power outage at the receiver. The power grid disruption begins ~8 seconds after the arrival of the s-waves at the receiver, and so may have been timed with the arrival of the s-waves at a power station or more populated area, at some location which is ~25 km further from the epicenter compared to the Onagawa receiver.

[19] We similarly examined the data from three strong foreshock earthquakes, occurring on 09 March 2011 at 02:45:20, 18:16:16, and 18:44:38 UT, with magnitudes 7.3, 6.0, and 5.9, respectively, all with epicenters very close to the main Tohoku earthquake. We found no anomalous emissions or power line frequency disruptions similar to those observed for the main earthquake. Data from the aftershocks are not available, but it does appear that these various anomalies are unique to only the most powerful earthquake.

3.2. Broadband ELF

[20] Figure 5 shows spectrograms of the lower 1 kHz of data, in half hour periods, for the 3+ hours preceding the earthquake, with power line interference again removed, although a few power line artifacts remain due to the imperfect 50 Hz subtraction algorithm (such as one at ~04:08 UT, the weaker one at ~03:30 UT, and the impulses at the 5, 15, and 25 minute point of every spectrogram). Although the data after processing are reasonably quiet, there does not appear to be any anomalous emissions in the hours preceding the earthquake. We are not able to comment on the presence of ULF emissions, such as those reported by *Fraser-Smith et al.* [1990] in the 0.01–5 Hz range, as those frequencies are too far below the cutoff frequency of our instrument.

3.3. VLF Transmitters

[21] The VLF receiver also recorded amplitude and demodulated phase of narrowband VLF transmitter signals which originate from all over the globe. These narrowband data are saved continuously, and are available for many months preceding the earthquake. Four VLF transmitters had particularly strong signals at Onagawa, including transmitters in Japan (JJI, 22.1 kHz), Washington State (NLK, 24.8 kHz), Hawaii (NPM, 21.4 kHz), and Australia (NWC, 19.8 kHz).

[22] Figure 6 shows the amplitude data from these transmitters, as a function of date and time, covering 2011 prior

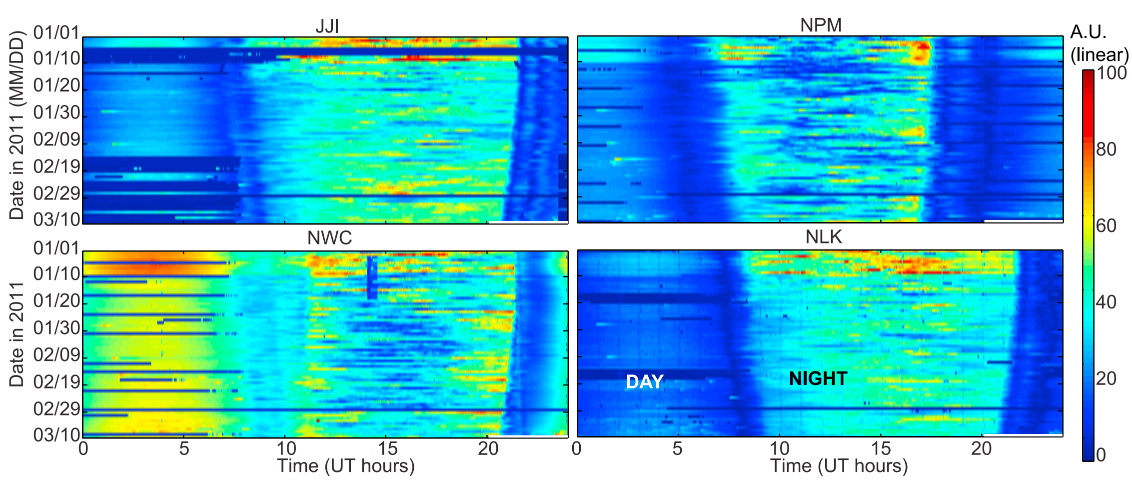

Figure 6. Record of narrowband transmitter amplitudes to the Onagawa receiver.

to the earthquake. In each panel, each row shows the amplitude of the signal during the course a single day; the days are stacked vertically, and the date is shown on the vertical axis. The sudden change in amplitude at 7–9 UT marks the change from a daytime to a nighttime ionosphere, and vice versa at 20–21 UT (17 UT for NPM). This is denoted as the day/night or night/day terminator. Thus, the central bright region marks nighttime in Japan; one can observe the ionospheric nights getting shorter from January to March.

[23] Previous work [*Hayakawa et al.*, 1997] argues that in the few days before the M7.2 earthquake in Kobe, Japan in 1995, the time of the terminators exhibited a large shift of over an hour, corresponding to an a lowering of the VLF reflection height by ~1.5 km. This was presented as a possible precursor signature to the large earthquake, potentially due to radon emissions from below the ground. That study used a short path between a transmitter at 10.2 kHz (part of the now defunct "Omega" system) and a receiver, with the earthquake was located on the path between transmitter and receiver. Subsequent studies have extended these results for long paths [*Hayakawa*, 2007; *Hayakawa et al.*, 2010], for paths over earthquakes below the sea [*Horie et al.*, 2007]. However, the data presented here shows no such precursory shift of the terminators, only the regular seasonal and diurnal shift, despite the incredible magnitude of the earthquake. The phase of the transmitter was separately examined and also shows no anomalous activity prior to the earthquake.

[24] One prominent study that failed to link transmitter amplitude or phase anomalies to earthquakes [*Clilverd et al.*, 1999] used long paths for which the earthquake was midway between the transmitter and receiver. Studies of localized lightning-induced disturbances have a shown a significant dependence on the transmitter-receiver geometry [*Marshall et al.*, 2006; *NaitAmor et al.*, 2010]. In particular, scattered higher-order waveguide modes from the ionospheric disturbance may not propagate to larger distances, so a receiver near the disturbance is more likely to detect it than a receiver for which the disturbance is halfway between the transmitter and receiver. So the case presented here may have been even more favorable for the detection of pre-seismic anomalies than those of *Clilverd et al.* [1999], and yet no associated anomaly was found. Other modeling efforts, based on lightning-generated heating, have shown that the distance from transmitter to receiver was in a good location for detecting perturbations from localized ionospheric disturbances [*Foust et al.*, 2011].

[25] **Acknowledgments.** This work was supported by intellectual curiosity, and by the sheer luck of having somehow acquired these measurements. We thank Tony Fraser-Smith for helpful discussions. Earthquake information was taken from the United States Geological Survey website. We thank Yukuhiro Takahashi, Tohoku University, and Hokkaido University for maintaining the receiver since its installation, and collecting the hard drive after the earthquake.

[26] The Editor thanks Craig Rodger and an anonymous reviewer for assisting in the evaluation of this paper.

References

Bordes, C., L. Jouniaux, M. Dietrich, J.-P. Pozzi, and S. Garambois (2006), First laboratory measurements of seismo-magnetic conversions in fluid-filled Fontainebleau sand, *Geophys. Res. Lett.*, *33*, L01302, doi:10.1029/2005GL024582.

Clilverd, M. A., C. J. Rodger, and N. R. Thomson (1999), Investigating seismoionospheric effects on a long subionospheric path, *J. Geophys. Res.*, *104*(A12), 28,171–28,179.

Cohen, M. B., U. S. Inan, and E. P. Paschal (2010a), Sensitive broadband ELF/VLF radio reception with the AWESOME instrument, *IEEE Trans. Geosci. Remote Sens.*, *48*(1), 3–17, 10.1109/TGRS.2009.2028334.

Cohen, M. B., R. K. Said, and U. S. Inan (2010b), Mitigation of 50–60 Hz power line interference in geophysical data, *Radio Sci.*, *45*, RS6002, doi:10.1029/2010RS004420.

Foust, F. R., M. Spasojevic, T. F. Bell, and U. S. Inan (2011), Modeling scattering from lightning-induced ionospheric disturbances with the discontinuous Galerkin method, *J. Geophys. Res.*, *116*, A12301, doi:10.1029/2011JA016973.

Fraser-Smith, A. C., A. Bernardi, P. R. McGill, M. E. Ladd, R. A. Helliwell, and O. G. Villard Jr. (1990), Low-frequency magnetic field measurements near the epicenter of the Ms 7.1 Loma Prieta earthquake, *Geophys. Res. Lett.*, *17*(9), 1465–1468.

Goghberg, M. B., V. A. Morgounov, T. Yoshino, and I. Tomizawa (1982), Experimental measurement of electromagnetic emissions possibly related to earthquakes in Japan, *J. Geoophys. Res.*, *87*, 7824–7828.

Gokhberg, M. B., I. L. Gufeld, A. A. Rozhnoy, V. F. Marenko, V. S. Yampolsky, and E. A. Ponomarev (1989), Study of seismic influence on the ionopshere by super long-wave probing of the Earth-ionosphere waveguide, *Phys. Earth Planet. Inter.*, *57*, 64–67.

Hayakawa, M. (2007), VLF/LF radio sounding of ionospheric perturbations associated with earthquakes, *Sensors*, *7*, 1141–1158.

Hayakawa, M., O. A. Molchanov, T. Ondoh, and E. Kawai (1997), On the precursory signature of Kobe earthquake on VLF subionospheric signals, in *International Symposium on Electromagnetic Compatibility Proceedings*, pp. 72–75, Inst. Electr. and Electron. Eng., New York.

Hayakawa, M., Y. Kasahara, T. Nakamura, F. Muto, T. Horie, S. Maekawa, Y. Hobara, A. A. Rozhnoi, M. Solovieva, and O. A. Molchanov (2010), A statistical study on the correlation between lower ionospheric perturbations as seen by subionospheric VLF/LF propagation and earthquakes, *J. Geophys. Res.*, *115*, A09305, doi:10.1029/2009JA015143.

Horie, T., T. Yamauchi, M. Yoshida, and M. Hayakawa (2007), The wave-like structures of ionospheric perturbation associated with Sumatra earthquake of 26 December 2004, as revealed from VLF observation in japan of NWC signals, *J. Atmos. Sol. Terr. Phys.*, *69*, 1021–1028.

Kennett, B. L. N., and E. R. Engdahl (1991), Travel times for global earthquake location and phase identification, *Geophys. J. Int.*, *105*, 429–465.

Marshall, R. A., U. S. Inan, and W. A. Lyons (2006), On the association of early/fast very low frequency perturbations with sprites and rare examples of VLF backscatter, *J. Geophys. Res.*, *111*, D19108, doi:10.1029/2006JD007219.

Molchanov, O. A., and M. Hayakawa (1999), Subionospheric VLF signal perturbations possibly related to earthquakes, *J. Geophys. Res.*, *103*, 17,489–17,504.

NaitAmor, S., M. A. AlAbdoadaim, M. B. Cohen, B. R. T. Cotts, S. Soula, O. Chanrion, T. Neubert, and T. Abdelatif (2010), VLF observations of ionospheric disturbances in association with TLEs from the EuroSprite-2007 campaign, *J. Geophys. Res.*, *115*, A00E47, doi:10.1029/2009JA015026.

Němec, F., O. Santolík, and M. Parrot (2009), Decrease of intensity of ELF/VLF waves observed in the upper ionosphere close to earthquakes: A statistical study, *J. Geophys. Res.*, *114*, A04303, doi:10.1029/2008JA013972.

Parrot, M., and M. M. Mogilevskii (1989), VLF emissions associated with earthquakes and observed in the ionosphere and magnetosphere, *Phys. Earth Planet. Inter.*, *57*, 86–99.

Rodger, C. J., N. R. Thomson, and R. L. Dowden (1996), A search for ELF/VLF activity associated with earthquakes using ISIS satellite data, *J. Geophys. Res.*, *101*(A6), 13,369–13,378.